Regression from pathological hypertrophy in mice is sexually dimorphic and stimulus-specific

Muehleman D.L., Crocini C., Swearingen A.R., Ozeroff C.D., Leinwand L.A.

American Journal of Physiology: Heart and Circulatory Physiology
2022 MAY; 322(5): H785-H797
2022 MAR 18 (first published online)
DOI: 10.1152/ajpheart.00644.2021

Publisher: American Physiological Society

Regression from pathological hypertrophy in mice is sexually dimorphic and stimulus-specific

Deanna L. Muehleman[1,2,*], Claudia Crocini[1,2,3,4*], Alison R. Swearingen[2], Christopher D. Ozeroff[1,2], Leslie A. Leinwand[1,2]

[1]BioFrontiers Institute University of Colorado Boulder, Boulder, USA, [2]Department of Molecular and Cellular Development, University of Colorado Boulder, Boulder, USA, [3]Max Delbrück Center for Molecular Medicine in the Helmholtz Association (MDC), Neuromuscular and Cardiovascular Cell Biology, Berlin, Germany, [4]German Center for Cardiovascular Research (DZHK) Partner Site Berlin, Berlin, Germany

* These authors contributed equally

Abstract

Pathological cardiac hypertrophy is associated with increased morbidity and mortality. Understanding the mechanisms whereby pathological cardiac growth can be reversed could be of therapeutic value. Here, we show that pathways leading to regression of pathological cardiac hypertrophy are strongly dependent on the hypertrophic trigger and are significantly modified by sex. Two pathological stimuli causing hypertrophy via distinct pathways were administered to male and female mice: Angiotensin II [Ang II] or Isoproterenol [Iso]. Stimuli were removed after 7 days of treatment, and left ventricles (LV) were studied at 1, 4, and 7 days. Ang II-treated Females did not show regression after stimulus removal. Iso treated males showed rapid LV hypertrophy regression. Somewhat surprisingly, RNAseq analysis at day 1 after removal of triggers revealed only 45 differentially regulated genes in common among all the groups, demonstrating distinct responses. Ingenuity Pathway Analysis predicted strong downregulation of the TGFβ1 pathway in all groups except for Ang II-treated females. Consistently, we found significant downregulation of Smad signaling after stimulus removal including in Ang II-treated females. Additionally, the ERK1/2 pathway was significantly reduced in the groups showing regression. Finally, protein degradation pathways were significantly activated only in Iso-treated males at 1 day after stimulus removal. Our data indicate that TGFβ1 downregulation may play a role in the regression of pathological cardiac hypertrophy via downregulation of the ERK1/2 pathway and activation of autophagy and proteasome activity in Iso-treated males. This work highlights that the reversal of pathological hypertrophy does not utilize universal signaling pathways and that sex potently modifies this process.

New & Noteworthy

Pathological cardiac hypertrophy is a major risk factor for mortality and is thought to be largely irreversible in many individuals. While cardiac hypertrophy itself has been studied extensively, very little is understood about its regression. It is important that we have a better understanding of mechanisms leading to regression, why this process is not reversible in some individuals and that sex differences need to be taken into account when contemplating therapies.

1. Introduction

Cardiac hypertrophy is a major risk factor for mortality and can be caused by high blood pressure, diabetes, mutations in sarcomeric proteins, and aortic valve stenosis (1-4). In mammals, this hypertrophy is the result of increased cardiomyocyte size, leading to thickening of the left ventricular (LV) walls and a decrease in the volume of the LV chamber. If cardiac hypertrophy persists for an extended time, there can be many maladaptive changes to the myocardium including: cell death, fibrosis and lengthening and thinning of the cardiomyocytes, ultimately leading to cardiac dilation and potentially, heart failure (5). In early stages of cardiac hypertrophy, the increase in cardiomyocyte size is compensatory to normalize ventricular wall stress; with early treatment of the underlying cause, cardiac hypertrophy can be reversed. However, there are varying degrees of regression of LV hypertrophy in hypertensive patients based on the treatment they receive (6). Angiotensin II (Ang II) receptor antagonists, calcium channel antagonists and angiotensin converting enzyme inhibitors can significantly decreased LV mass index by: 13%, 11% and 10%, respectively (6). However, diuretics and β-adrenergic receptor blockers did not affect LV mass index (6). In addition, weight loss and decreased sodium intake led to similar decreases in LV mass index compared to patients that received anti-hypertensive drug treatments (7). Following aortic valve replacement for aortic stenosis, patients experienced LV mass reductions ranging from 17%-31%, and these changes were strongly associated with the severity of LV hypertrophy before surgery (4). Overall, the longer the heart experienced a pathological stress and the increased work load,, the more maladaptive changes occurred, and hypertrophy was less likely to be reversible (5, 8). There are notable cases in which regression of chronic pathological cardiac hypertrophy occurred more readily, including bariatric surgery in which significant decreases in LV mass ranged from 21%-30% (9-12) or a Left Ventricular Assist Device (LVAD) in which significant decreases in LV mass ranged from 28%-41% (13, 14). While many mechanisms that lead to cardiac hypertrophy are known, very little is understood about regression of cardiac hypertrophy.

Models for regression of cardiac hypertrophy include a de-banding from transverse aortic constriction (TAC)(15-19), or the removal of a hypertrophic agonist such as Ang II or Iso (20-22). Each of these models demonstrated regression after approximately 7 days, and there was a return to baseline of pathologic gene expression markers such as atrial natriuretic factor (ANF)(18, 20, 22), brain natriuretic peptide (BNP)(17), collagen 1A(17) and a normalization of the functional response such as ejection fraction (17, 19) and cardiac output (19, 21). However, each of these studies only reported a single timepoint after which regression was already complete. In addition, while one group reported a possible state of irreversible

hypertrophy with one week of de-banding after chronic TAC (6 weeks), there was still a reversal of pathological gene expression including, *Myh7* and *Acta-1* (17). However, the rate of regression, and the many molecular mechanisms that occur during the process of regression, are still unknown. A better understanding of the immediate responses and the progression of regression, along with a model of incomplete hypertrophy regression, will be important to understand why some patients experience regression and others do not. Finally, sex differences in regression have not been adequately addressed.

Sex differences in cardiac diseases have been observed for many years now, with some differences observed in the rates and extent of hypertrophy and/or regression. For example, with aortic stenosis, although women experienced cardiac hypertrophy more often, and to a greater extent, they also regressed from hypertrophy faster than men (23). In addition, males had higher expression of collagen I & III and matrix metalloproteinase 2 genes due to aortic stenosis, which may be a factor contributing to the slower rates of regression in males (23, 24). In the studies of LVAD placement, while some of the patients receiving an LVAD were female, most were males (13, 14, 25). Although sex was accounted for in the demographics, sexes were combined when analyzing LV mass differences and molecular changes. Similarly, patients receiving bariatric surgery were primarily female, but sexes were combined when analyzing results. However, there was one study that showed male sex was independently associated with an increase in the 1-year mortality rate post-bariatric surgery (26). In rodent models of regression of hypertrophy, de-banding from TAC or removal of the hypertrophic agonist (Ang II or Iso), were carried out with either only male rodents (16, 17, 20-22), the sex was not stated (18), or the results of the sexes were combined (15). We are just beginning to understand the many molecular mechanisms that underlie sex differences, even at baseline (27). Therefore, it is essential to define sexually dimorphic cardiac differences, both at baseline, and in response to stress.

Here, we compare cardiac hypertrophy and regression induced by two different pathological hypertrophic stimuli, Ang II or Iso in male and female mice. In addition, we compare the sexes at baseline for many cardiac parameters and find significant differences. Although both agonists caused hypertrophy, the extent of regression of hypertrophy was distinct between the sexes and the agonists. There were differences in transcriptome, activation of signaling pathways, extracellular matrix composition, and protein degradation pathways depending on the hypertrophic stimulus and/or biological sex. Furthermore, there we very few genes regulated in common among the groups.

2. Methods

2.1 Animals and treatments. All animal treatments were approved by the Institutional Animal Care and Use Committee at the University of Colorado Boulder (Protocol #2351) and are in accord with the NIH guidelines. Wild-type, 10-12-week-old C57Bl/6 male and female mice (Jackson Laboratories) were fed *ad libitum* standard rodent chow and housed in a 12-hour light/dark cycle. Mice were treated with Ang II (2.88mg/kg/day) or Iso (30mg/kg/day) for 7 days (Figure 1A). Ang II was diluted in sterile saline. Iso was prepared in 1μM Ascorbic Acid, diluted in sterile saline. Ang II and Iso were released through osmotic mini-pumps (Alzet model 2001). Mice were anaesthetized with Isoflurane (3%) via spontaneous inhalation. Surgical procedures were performed on a 37°C re-circulated heating pad. The analgesic buprenorphine was used at 1mg/kg. To study regression, the osmotic pumps were removed after 7 days of Ang II/Iso; the same surgical procedure was used as placement of the mini-pump. Mice were euthanized by first anaesthetizing with Isoflurane (3%) via spontaneous inhalation, then the heart was removed. Mice were sacrificed at either 7 days of Ang II/Iso, indicating peak hypertrophy, or at Post-Stimulus Day 1, 4 & 7 (P1, P4 & P7 respectively) (Figure 1A). Hypertrophy was determined as the ratio of the mass of LV + septum over tibia length (LV/TL). There were vehicle controls (1μM Ascorbic Acid in sterile saline for Iso or sterile saline alone for Ang II) at each timepoint. Hearts were dissected, and the left ventricle was weighed then flash frozen in liquid nitrogen. Tissue was placed at -80C until further analysis.

2.2 Protein Isolation & Western Blots. LV tissue was homogenized in Urea Buffer (8M Urea, 2M Thiourea, 50mM Tris (pH 6.8), 75mM DTT, 3% SDS, 0.05% Bromophenol Blue). Protein concentration was determined using Pierce 600 Protein Assay Reagent (Thermo Scientific 22660) with the Pierce Ionic Detergent Compatibility Reagent (Thermo Scientific 22663). Proteins were run on 4-12% Bis-Tris gels and transferred to Nitrocellulose membranes. Membranes were blocked with 5% BSA in TBST (TBS + 0.1% Tween) for 1 hour at room temperature. Primary antibodies were incubated O/N in 5% BSA (TBST) at 4°C. Secondary antibodies were incubated for 1 hour at room temperature. Membranes were imaged using ECL reagent (Perkin-Elmer NEL104001EA). Quantification was determined using ImageQuant. All primary antibodies were purchased through Cell Signaling Technology and used at a 1:1000 dilution: p-SMAD2 (3108), p-Akt (4058), p-p38 (4511), p-ERK1/2 (9101), LC3 (2775), except α-Vinculin, purchased from Sigma (V9131). Secondary antibodies HRP-conjugated anti-mouse (Jackson ImmunoResearch) or anti-rabbit (Cell Signaling Technology) were used at 1:5000 dilutions.

2.3 Proteasome Activity Assay. Left ventricle tissue was homogenized in Proteasome buffer (50mM HEPES; 20mM KCl; 5mM MgCl2; 1mM DTT). Samples were centrifuge at 10,000xg for 30 minutes at 4°C. The supernatant was placed in a new tube and the protein concentration was determined using Pierce BCA Protein Assay (Thermo Scientific 23227). Each reaction contained 15µg protein in a final volume of 230µl Proteasome buffer. In addition, each sample had a complimentary reaction which contained the proteasome inhibitor MG132 (20nM). 230µl of the sample was prepared on a 96-well white flat bottom plate. 10µl of the fluorescent substrate was added; Suc-LLVY-AMC was used to measure chymotrypsin activity (18µM; Enzo Life Sciences BML-P802). The samples were kept on ice until this point. The reaction was started by placing the plate in the plate reader at 37°C and fluorescence was measured every 3 minutes for 60 minutes (excitation 360nm; emission 460nm). Proteasome activity was determined by calculating the change in fluorescence; this value was then subtracted from the change in fluorescence from the complimentary reaction containing MG132. Each sample was run in triplicates.

2.4 RNA isolation. LV tissue was homogenized in Tri Reagent (Molecular Research Center, TR118). Chloroform was added and incubated at room temperature for 15 minutes, then centrifuged at 12,000xg for 15 minutes at 4°C. The aqueous layer was removed and placed in a new tube. Isopropanol was added and incubated at room temperature for 15 minutes, then centrifuged at 12,000xg for 15 minutes at 4°C. The supernatant was removed, and the pellet was washed with 70% ethanol, then centrifuged at 7,500xg for 5 minutes at 4°C. The supernatant was removed, and the RNA was resuspended in water.

2.5 RNAseq preparation and analysis.

RNA samples were submitted to Novogene for library preparation, by PolyA selection, and sequencing. All samples had a sequencing depth of at least 20 million 150 bp paired end reads. All differential expressed gene (DEG) analyses were carried out in R (version 3.5.0) with Bioconductor (3.10) package edgeR (3.10.2). Reads were removed from analysis if expression was less than 0.5 counts per million. Data was fit using glmRTFit function. P-values were adjusted by the Benjamini-Hochberg method to control False Discovery Rate (FDR) at 0.05. Once exclusively DEGs were identified, we used QIAGEN Ingenuity Pathway Analysis (IPA) software for identifying predicted functional pathways and upstream regulators.

2.6 cDNA preparation and Quantitative Real-Time PCR. RNA was reverse transcribed using SuperScript III Reverse Transcriptase (Invitrogen 18080044) and the protocol was followed according to the manufacture. cDNA was diluted to 1µg/ul in water. Each QPCR reaction contained, 4µg cDNA + SYBR Green PCR Master Mix (Invitrogen 4309155) + 12.5µM primer set. Thermocycler settings were determined used SYBR Green PCR Master Mix Protocol. ΔΔCt was calculated using 18S as a normalizer.

Primer	Forward	Reverse
18S	GCCGCTAGAGGTGAAATTCTTG	CTTTCGCTCTGGTCCGTCTT
Col1a1	TACCGCTGGAGAACCTGGAA	GGGACCTTGTACACCACGTT
Postn	AAGTTTGTTCGTGGCAGCAC	TGTTTCTCCACCTCCTGTGG

2.7 Hydroxyproline Assay. A hydroxyproline assay kit was used (Sigma-Aldrich; MAK008) and followed according to the manufacturer's instructions. Briefly, 10mg of tissue was homogenized, then hydrolyzed in 12M HCl. 30µl of each sample was transferred in duplicate to a 96 well plate and allowed to dry in a 60°C oven for 60 minutes. Chloramine T/Oxidation Buffer was added to each sample and standard well, followed by the diluted DMAB Reagent. Samples were incubated for 90 minutes at 60°C. Absorbance was measured at 560nm.

2.8 Statistical Analysis. Statistical differences were determined between two groups using Student's two-tailed T-test. Between multiple groups, one-way ANOVA was performed followed by Uncorrected Fisher's LSD post-hoc test. Outliers were determined using the Grubbs test with an $\alpha<0.05$. P-values of less than 0.05 were considered significant.

3. Results

3.1 Pathological cardiac hypertrophy and regression. In order to determine whether a pathological response to different stimuli would show similar patterns of hypertrophy and regression, we treated male and female C57/Bl6 mice with an activator of the Renin-Aldosterone-Angiotensin-System (RAAS), Ang II, or the β-adrenergic agonist, Iso, to induce a pathological cardiac remodeling and hypertrophy. After 7 days, treatments were removed and hearts were analyzed at different timepoints to investigate regression of cardiac hypertrophy (Figure 1A). Male mice treated with Ang II (2.88mg/kg/day) experienced an increase of 25.6% in LV/TL (Figure 1B, Supplemental Figure 1A), and female mice

experienced an increase of 32.7% in LV/TL (Figure 1B, Supplemental Figure 1B), but these sex differences were not statistically significant. Iso treatment (30mg/kg/day) induced a 33.8% increase in LV/TL in males (Figure 1B, Supplemental Figure 1A). Female mice showed a 28.5% increase in LV/TL (Figure 1B Supplemental Figure 1B). Although this male-female difference was not statistically significant, it corroborates an earlier study that showed females have a more modest hypertrophic response to Iso treatment (28).

After removal of hypertrophic stimuli, mice showed significantly different rates of regression. After Ang II was removed, neither males nor females showed any significant regression at P1 and, although male hearts regressed significantly at P4 (Figure 1B, Supplement Figure 1A-B), the LV weights of both males and females, remained significantly larger (approximately 20%) than the vehicle controls at P7, demonstrating incomplete regression. Iso male mice regressed faster than all other groups (Figure 1A). Regression was significant already after 1 day (P1) of Iso removal in male mice and they showed complete regression after 4 days (P4) as compared to the vehicle control (Figure 1A). After Iso was removed, female mice showed significant, but incomplete regression immediately at P1, similar to males (Figure 1B). However, Iso females exhibited a slower regression and only showed complete regression at P7 (Fig 1B, Supplement Figure 1). This is the first report to investigate the immediate response, and the rates of regression with two different models, including one that is irreversible at the timepoints studied here, in addition to examining biological sex as a variable.

3.2 RNAseq revealed sex- and trigger dependent gene expression responses to removal of the hypertrophic stimulus.

Considering the slow and incomplete regression from Ang II, and the fast regression response of male and female mice after Iso treatment, we investigated the cardiac transcriptomes of all experimental groups after hypertrophy and at P1 of regression. We performed RNAseq and assessed gene expression differences elicited by removal of hypertrophic stimuli (Figure 1C). After Ang II removal, males showed 831 differentially expressed genes while females showed 2063 genes differentially regulated (Figure 1D). In Iso males, 1152 genes were differentially expressed when comparing P1 to Hypertrophy, while Iso females showed only 340 differentially expressed genes (Figure 1D). This result was unexpected considering that removal of Ang II induced little regression of cardiac hypertrophy in either male or female mice. Moreover, these large responses of the transcriptome after removal of the hypertrophic trigger suggest that the heart is responding strongly in Ang II treated mice, although not culminating in regression.

Of note, only 45 differentially expressed genes were in common among all regression groups (Figure 1D, Supplement Figure 2), suggesting that the removal of hypertrophic stimulus triggers largely distinct responses IPA canonical pathways analysis

of the 45 common genes identified two enriched pathways both related to cell cycle control (Figure 1F). However, the vast majority of common genes did not cluster into enriched pathways. Thus, our data indicate distinct transcriptional profiles associated with removal of hypertrophic stimuli that depend on the nature of the hypertrophic trigger and biological sex.

3.3 Fibrotic signaling is inactivated during regression of cardiac hypertrophy but fibrosis increases.

For each group, we then performed IPA canonical pathways analysis on differentially expressed genes between P1 and Hypertrophy. Results of the analyses were compared among groups to identify shared and distinct signaling pathways (Figure 2A, Supplemental Figure 3). All groups exhibited similar downregulation of cell cycle and proliferation signaling at P1 with the exception of female Ang II. Male Iso also showed a higher degree of downregulation of fibrosis signaling (identified as *hepatic fibrosis signaling*) and cardiac hypertrophy signaling as compared to all the other groups. IPA prediction of upstream regulators identified TGF-β1 inhibition in male Iso at P1 as the most significant regulation among all groups (Figure 2B). In male Iso, 248 differentially-expressed genes were associated with inhibition of TGF-β1, including numerous fibrotic genes downregulated at P1 as compared to hypertrophy (Figure 2C). The formation of a fibrotic network in the myocardium may play a role in the ability to regress following a pathological stress. We therefore measured hydroxyproline content with the hypothesis that higher collagen levels would inhibit or reduce regression, especially in male male and female Ang II that showed the least regression (Figure 1B). Unexpectedly, collagen content was not increased in hypertrophy for any of the groups and showed a similar increasing trend after removal of the hypertrophic trigger in all of the groups. Hydroxyproline content was significantly increased by P4 in both Ang II and Iso males (Figure 2D) as compared to vehicle control mice, while in female Ang II, the increase was significant only at P7. Collagen content in female Iso did not reach statistical significance by 7 days after removal of the trigger even though regression was complete at that time point. We predicted that the (re)activation of fibrotic genes during regression was the cause of increased fibrosis, therefore we measured the expression of Collagen1 a1 (*Col1a1*) and Periostin (*Postn*), both of which are components of the extracellular space and contribute to fibrotic networks (29). Interestingly, both *Col1a1* and *Postn* were increased in hypertrophy for all of the groups (Supplemental figure 4) and progressively reduced with removal of the hypertrophic trigger, with the exemption of female Ang II that maintained higher expression level of both genes at P1. Overall, female Iso showed the smallest increase in expression of *Col1a1* and *Postn* in hypertrophy and a significant downregulation of both genes at P1. The same group showed only a mild non-significant increase of hydroxyproline content at P7. Of note,

hydroxyproline content and *Col1a1* expression were higher at baseline in females as compared to males, with no difference in the expression of *Postn* (Supplemental figure 5A). These data together indicate that collagen content is sexually dysmorphic at baseline and that expression of fibrotic genes depends on the hypertrophic trigger although fibrosis can be manifested at later times even after the removal of the hypertrophic signal and during cardiac regression.

3.3 TGF-β1 canonical and non-canonical pathways.

TGF-β1 signals through Ser/Thr kinase receptors that activate a canonical pathway by phosphorylating Smad2/3 (small mother against decapentaplegic), and non-canonical pathways via PI3K/AKT, Ras/ERK, and MEKK/p38 (Figure 3A). Phosphorylated Smad2/3 forms homomeric and heteromeric SMAD complexes that translocate to the nucleus and induce a fibrotic gene program (30, 31). We first evaluated the baseline levels for SMAD signaling and the TGF-β1 non-canonical pathways between males and females (Supplementary figure 5B). Activation of p-SMAD2/3 was not different between males and females, suggesting that the higher levels of *Col1a1* observed in females was not the result of a specific signaling but rather the healthy baseline levels associated with female biological sex. Conversely, Akt and ERK1/2 signaling were both higher in females as compared to males (Supplementary figure 5B). There was no sex difference in p-p38 at baseline (Supplementary figure 5B). Significant activation of p-Smad2/3 was observed in all groups in hypertrophy as compared to vehicle, in good agreement with gene expression levels of *Col1a1* and *Postn* (Supplemental figure 4A-B). At P1, consistent with gene expression and RNAseq data showing downregulation of genes downstream of the TGF-β1/Smad pathway (Figure 2C), p-Smad2/3 was significantly decreased in Iso treated males and females. It was significantly decreased at P4 in Ang II treated males, and remained elevated in Ang II treated females (Figure 3B), also in agreement with *Col1a1* and *Postn* gene expression. Overall, Ang II infusion for 7 days resulted in longer activation of Smad2/3 as compared to Iso infusion, and extended beyond the removal of the hypertrophic trigger (Figure 3B). Akt phosphorylation (Ser473) was significantly inactivated only in Iso females at P1, although it was not increased with Iso treatment as compared to vehicle control (Figure 3C). p38 signaling (phosphorylation on Thr180 and Tyr182) was moderately but significantly reduced only in Ang II males at P1as compared to hypertrophy, although it was not significantly different in hypertrophy as compared to vehicle control (Figure 3D). Finally, ERK1/2 signaling (Thr202/Tyr204) was significantly activated in males treated with Ang II or Iso and significantly inactivated in both groups at P1 (Figure 3E). At P1, Iso females also showed significant

inactivation of ERK pathway, although they did not exhibit a significant activation of ERK in hypertrophy as compared to vehicle (Figure 3E).

3.4 Protein degradation pathways are differentially regulated by sex and the hypertrophic trigger.

Considering that during cardiac hypertrophy there is an increase in protein synthesis (32), we hypothesized that protein degradation pathways, namely the ubiquitin proteasome system and autophagy, would be regulated in order to promote regression and degrade proteins that accumulated during hypertrophy. Proteasome activity was determined by incubating lysates with the proteasome chymotrypsin-like substrate, Suc-LLVY-AMC (33). First, we observed that there were no differences in proteasome activity between males and females at baseline (Supplemental Figure 5C). We found that proteasome activity increased with both Ang II and Iso in male mice at hypertrophy; however, the increase was larger in Ang II treated mice (Figure 4A). While proteasome activity decreased immediately following the removal of Ang II, the removal of Iso resulted in a significant further increase, suggesting it may be involved in protein turnover in both hypertrophy and regression (Figure 4A). By P4, the time point of complete regression, male Iso proteasome activity returned to baseline. In female mice, proteasome activity remained unchanged throughout hypertrophy and regression for both Ang II and Iso treatments (Figure 4A). We measured autophagy by quantitation of the two forms of LC3. LC3 is a small protein that becomes lipidated in the growing autophagosome and we measured the amount of the lipidated form (LC3II) relative to the unlipidated form (LC3I). At baseline, females had 2-fold more LC3II/LC3I, compared to males, indicating they had higher autophagic activity (Supplemental Figure 5C). Autophagy did not appear to be activated by Ang II-induced hypertrophy or during regression in male or female mice. Autophagy increased in males and females at P1 following the removal of Iso. Iso females showed a significant reduction of autophagy during hypertrophy as compared to vehicle controls, possibly to promote accumulation of proteins. Additionally, removal of Iso activated autophagy in females at P1 and remained higher at P4 and P7 as compared to the hypertrophy time point (Figure 4B), but it was not different than baseline levels measured in vehicle controls. These results indicate that mice treated with Iso may regress at higher rates than Ang II treated groups via induction of autophagy.

4. Discussion

Pathological cardiac hypertrophy is a risk factor for mortality and can be reversed with pharmacological treatment, weight loss or surgery in some patients; however, not all patients respond to treatment by regressing their hypertrophy (1, 4, 6-8). The primary aim of our study was to determine whether sex and/or the nature of the pathological trigger impact regression differently. We induced hypertrophy in male and female mice with two different pathological agonists, Ang II and Iso, and studied gene expression programs and signaling pathways following the removal of the agonists. We showed that early after removal of pathological triggers, distinct gene expression profiles were elicited and that regression was dependent both on sex and pathological trigger.

Ang II and Iso are known to act through different pathways converging on cardiac hypertrophy. Ang II is the main effector in the RAAS, and binds to Ang II receptors (AT1R) (34). Ang II induces inflammation along with many pathological hypertrophic markers (NF-κB, TNFα, MAPK & Akt signaling), which ultimately leads to an increase in blood pressure (34) and cardiac hypertrophy. Iso activates adrenergic receptors that are a class of G-protein coupled receptors on the cell surface that cause a canonical signaling cascade leading to increased concentration of Ca^{2+} in the cytosol (35). This increase ultimately results in faster contractions of the cardiomyocytes and mimics the increased work-load observed in the disease state. Increased adrenergic signaling via catecholamines can also lead to high blood pressure and hypertrophy. In fact, hypertensive patients can be effectively treated with adrenergic receptor antagonists (36). While Iso induces cardiac hypertrophy in the mouse strain (C57Bl/6), there are reports of less pathology (37) and little evidence of fibrosis (38, 39) compared to other mouse strains. In contrast, with Ang II, there has been evidence for pathological signaling and significant cardiac fibrosis (34, 40) in the C57Bl/6 background. A previous study in FVB mice compared the different rates of regression of heart weights between Iso and Ang II and showed that regression occurred from both stimuli (20). However, the timing and dosage of these experiments differ from our current study (20). In that work, Ang II was used at 200 ng/kg/min X 14 days; that is about 15 times less than our dosage for twice as long; and Iso was used at 15 mg/kg/day x 7 days; half of our treatment. Regression was then observed at7 days after Iso treatment and at 14 days after Angiotensin II. Additionally, the authors only investigated hypertrophy and regression in male mice. Our work provides the first comparison between male and female regression from pathological hypertrophy in either of these models.

In our work, hypertrophic responses were not significantly different between either agonist or sex (Figure 1B and Supplemental Figure 1A-B). However, regression showed both sex differences and agonist-specific differences (Figure 1B

and Supplemental Figure 1A-B). In response to Ang II withdrawal, males experienced a significant regression at P4 while female LV weights remained higher and did not regress within the experimental window of 7 days (Figure 1B and Supplemental Figure 1A-B). After withdrawal of Iso treatment, males completely regressed by 4 days, whereas it took females 7 days to completely regress (Figure 1B and Supplemental Figure 1A-B). A previous study showed that complete regression from Ang II-induced hypertrophy occurred after 7 days, but the mice were of different genetic background and the dose was lower than the one used in our study resulting in <20% of cardiac hypertrophy (20). Our work also shows significant differences in the rate of regression comparing males and females.

Using RNAseq, we compared gene expression of LVs at the hypertrophy timepoint and at day 1 after removal of the trigger in Iso and Ang II males and females. The magnitude of total gene expression changes only 24 hours after stimulus removal was much higher than we expected: 3458 genes significantly regulated with very little commonality shared by all 4 groups. Only 45 differentially-expressed genes were shared by all 4 groups (Figure 2D) after removal of the hypertrophic trigger of which only 4 and 5 genes clustered in cell cycle controls and kinetochore metaphase signaling pathways, respectively (Figure 1E). Also somewhat surprisingly, more than 2000 genes were differentially expressed in females following the removal of Ang II (compared to Ang II hypertrophy) (Figure 1C-D) despite the fact that this group did not show significant regression (Figure 1B and Supplemental Figure 1A). Analyzing the entire transcriptome of each group after removal of the hypertrophic trigger, we observed that male Iso showed higher downregulation of cardiac hypertrophy and fibrosis pathways (Figure 2A), as well as the most significant downregulation of TGFβ1 (Figure 2B). While fibrosis was not previously associated with Iso-treatment in mice (38, 39), we found remarkable downregulation of numerous fibrotic genes in our male Iso group (Figure 2C). These results led us to conclude that less fibrotic gene signaling in male Iso was likely to contribute to the faster regression observed in this group compared to the others. Additionally, previous studies showed that Ang II induces significant fibrosis (34, 40, 41), which we predicted was the underlying cause of irreversible hypertrophy observed in the Ang II groups. However, collagen content increased over time during regression in all groups and was significant 7 days after the removal of the trigger with the exception of female Iso. Gene expression of collagen (*Col1a1*) and periostin (*Postn*) was significantly decreased with removal of hypertrophic triggers in all groups except for female Ang II. These results showed a temporal disconnect between a fibrotic gene program and fibrosis that warrants further investigation. Recently, a study found that hypertrophy induced by Ang II was associated with increased TGFβ1, *Postn*, and *Col1a1* gene expression in both male and female mice that resulted in increased tissue fibrosis (41). These different results could be

explained by the different experimental design as compared to our work. McLellal *et al.*, used Ang II infusion (1.5 mg/kg/day) for 14 days, while we administered Ang II (2.88mg/kg/day) for 7 days. Of note, female hearts showed significantly higher levels of collagen deposition and *Col1a1* gene expression than males at baseline (Supplementary Figure 5A). Although the role of biological sex on cardiac function is still understudied (42), strong evidence indicates that sex dimorphism extends from whole heart function to myofibril mechanics (27) and exists in many if not all cardiac cell populations (43), including cardiac fibroblasts (44) that are largely responsible for collagen expression and deposition.

We followed-up on the predicted TGFβ1 inhibition by assessing the activation status of both canonical and non-canonical TGFβ1 pathways (Figure 3A). In line with the RNAseq analysis showing reduced expression of genes targeted by the TGFβ1/Smad pathway, we found that the Smad2/3 signaling pathway was inactivated in male and female Iso at P1 and in male Ang II at P4. It remained significantly activated in female Ang II (Figure 3B). Non canonical TGFβ1 pathways showed different levels of (in)activation among groups. There were no significant changes in p-Akt levels during Iso or Ang II induced hypertrophy in males. Female mice showed a very minimal decreased p-Akt levels during hypertrophy, with only a significant decrease of p-Akt in response to Ang II and the removal of Ang II (Figure 3C). None of the groups showed activation of the p38 pathway but the removal of the hypertrophic trigger elicited a significant decrease in male Ang II only. Finally, there was a significant increase in p-ERK1/2 during Ang II or Iso induced hypertrophy in males (Figure 3D) and no significant changes in female mice due to Ang II or Iso. Immediately following the removal of the stimulus, all male mice, and female Iso mice, experienced significant decreases in p-ERK1/2 (Figure 3A). Activation of ERK1/2 has been observed in many pathological models (45) and inhibition of p-ERK1/2 has been shown to inhibit cardiac hypertrophy (46, 47). Our work provides additional insights into the ERK pathway by demonstrating its rapid inactivation following the removal of a pathological stimulus, similarly to p-Smad2/3, in the groups that show hypertrophic regression.

We hypothesized the involvement of protein degradation pathways to promote regression of cardiac hypertrophy. At baseline, proteasome activity was not different between males and females, while significantly higher autophagy was observed in female hearts as compared to males (Supplementary Figure 5C). This result is consistent with a previous report claiming 50% higher LC3II levels in females as compared to males in C57Bl/6 (although the results were unpublished in the publication) (48). In males, proteasome activity increased with Iso treatment and further increased immediately after removal of Iso (Figure 4A). In contrast, Ang II resulted in a greater increase in proteasome activity compared to Iso;

however, the activity level was significantly reduced immediately following the withdrawal of Ang II at P1. These results indicate the proteasome may have an active role in regression from Iso induced hypertrophy, but not following the removal of Ang II, in male mice. There were no notable changes in proteasome activity in female mice (Ang II or Iso) (Figure 4A). Regarding the autophagy response to pathological hypertrophy, reports vary with some showing autophagy was increased (49), while others reported autophagy was decreased during early hypertrophy (50, 51), and then increased in failing hearts (51). However, each of these studies only reported on male rodents, and because autophagy is an important target for many pharmaceutical treatments, it is important to understand how autophagy is differently regulated in males and females in response to cardiac stressors. In our study, Iso did not induce autophagy in male mice, nor did Ang II in either sex. Female Iso showed instead decreased autophagy in hypertrophy (Figure 4B). After removal of Iso, autophagy increased in both males and females at P1 compared to the Iso hypertrophic state (Figure 4B). Some reports indicate autophagy can be an indicator of health, as autophagy tends to decrease with age and poor health (52). Further, when autophagy was promoted by caloric restriction, diastolic dysfunction was delayed in an aging rodent (53) whereas when autophagy was inhibited, cardiac function and structure declined (52). This could explain the faster regression observed in male and female Iso treated mice after removal of the hypertrophic trigger as compared to Ang II groups. Male Iso showed increases of both autophagy and the proteasome activity, following stimulus removal, possibly resulting in the fastest regression rate among all groups. We posit protein degradation pathways could be a determining factor in regulating regression of cardiac hypertrophy.

In conclusion, complete regression of pathological cardiac hypertrophy occurred in the Iso model in both sexes, but the rate of regression was slower in females. Incomplete regression occurred in the Ang II model in both biological sexes. These differences could be due to alterations in signaling pathways, fibrotic gene expression, or protein degradation pathways that appear to be influenced by the hypertrophic trigger and by the biological sex (Figure 5). Future studies will include probing more pathways to further understand regression, especially any sex differences that may affect how patients are treated and respond to anti-hypertensive treatments.

Funding: This work was supported by the Tom Marsico Endowment Fund and NIH Grant GM029090 to L.A.L. C.C was supported by the Human Frontiers Science Program fellowship (LT001449/2017-L) and by the American Heart Association postdoctoral fellowship (20POST3521111).

Acknowledgements: We would like to thank Dr. Angela Peter for helpful discussions.

The authors have no conflicts of interest.

Supplementary figures available at https://doi.org/10.6084/m9.figshare.19314041.v1

References

1. **Aronow WS**. Hypertension and left ventricular hypertrophy. *Annals of translational medicine* 5: 310, 2017.
2. **Eguchi K, Boden-Albala B, Jin Z, Rundek T, Sacco RL, Homma S, and Di Tullio MR**. Association between diabetes mellitus and left ventricular hypertrophy in a multiethnic population. *The American journal of cardiology* 101: 1787-1791, 2008.
3. **Marian AJ, and Braunwald E**. Hypertrophic Cardiomyopathy: Genetics, Pathogenesis, Clinical Manifestations, Diagnosis, and Therapy. *Circulation research* 121: 749-770, 2017.
4. **Rader F, Sachdev E, Arsanjani R, and Siegel RJ**. Left ventricular hypertrophy in valvular aortic stenosis: mechanisms and clinical implications. *The American journal of medicine* 128: 344-352, 2015.
5. **Wang Y**. Signal transduction in cardiac hypertrophy--dissecting compensatory versus pathological pathways utilizing a transgenic approach. *Current opinion in pharmacology* 1: 134-140, 2001.
6. **Klingbeil AU, Schneider M, Martus P, Messerli FH, and Schmieder RE**. A meta-analysis of the effects of treatment on left ventricular mass in essential hypertension. *The American journal of medicine* 115: 41-46, 2003.
7. **Liebson PR, Grandits GA, Dianzumba S, Prineas RJ, Grimm RH, Jr., Neaton JD, and Stamler J**. Comparison of five antihypertensive monotherapies and placebo for change in left ventricular mass in patients receiving nutritional-hygienic therapy in the Treatment of Mild Hypertension Study (TOMHS). *Circulation* 91: 698-706, 1995.
8. **van Straten AHM, Soliman Hamad MA, Peels KCH, van den Broek KC, ter Woorst JFJ, Elenbaas TW, and van Dantzig J-M**. Increased Septum Wall Thickness in Patients Undergoing Aortic Valve Replacement Predicts Worse Late Survival. *The Annals of Thoracic Surgery* 94: 66-71, 2012.
9. **Jhaveri RR, Pond KK, Hauser TH, Kissinger KV, Goepfert L, Schneider B, Jones DB, and Manning WJ**. Cardiac remodeling after substantial weight loss: a prospective cardiac magnetic resonance study after bariatric surgery. *Surgery for obesity and related diseases : official journal of the American Society for Bariatric Surgery* 5: 648-652, 2009.
10. **Luaces M, Cachofeiro V, García-Muñoz-Najar A, Medina M, González N, Cancer E, Rodríguez-Robles A, Cánovas G, and Antequera-Pérez A**. Anatomical and Functional Alterations of the Heart in Morbid Obesity. Changes After Bariatric Surgery. *Revista Española de Cardiología (English Edition)* 65: 14-21, 2012.
11. **Valezi AC, and Machado VH**. Morphofunctional evaluation of the heart of obese patients before and after bariatric surgery. *Obesity surgery* 21: 1693-1697, 2011.
12. **Algahim MF, Lux TR, Leichman JG, Boyer AF, Miller CC, 3rd, Laing ST, Wilson EB, Scarborough T, Yu S, Snyder B, Wolin-Riklin C, Kyle UG, and Taegtmeyer H**. Progressive regression of left ventricular hypertrophy two years after bariatric surgery. *The American journal of medicine* 123: 549-555, 2010.
13. **Zafeiridis A, Jeevanandam V, Houser SR, and Margulies KB**. Regression of cellular hypertrophy after left ventricular assist device support. *Circulation* 98: 656-662, 1998.
14. **Altemose GT, Gritsus V, Jeevanandam V, Goldman B, and Margulies KB**. Altered myocardial phenotype after mechanical support in human beings with advanced cardiomyopathy. *The Journal of heart and lung transplantation : the official publication of the International Society for Heart Transplantation* 16: 765-773, 1997.
15. **Gao XM, Kiriazis H, Moore XL, Feng XH, Sheppard K, Dart A, and Du XJ**. Regression of pressure overload-induced left ventricular hypertrophy in mice. *American journal of physiology Heart and circulatory physiology* 288: H2702-2707, 2005.
16. **Stansfield WE, Charles PC, Tang RH, Rojas M, Bhati R, Moss NC, Patterson C, and Selzman CH**. Regression of pressure-induced left ventricular hypertrophy is characterized by a distinct gene expression profile. *The Journal of thoracic and cardiovascular surgery* 137: 232-238, 238e231-238, 2009.

17. **Andersen NM, Stansfield WE, Tang RH, Rojas M, Patterson C, and Selzman CH**. Recovery from decompensated heart failure is associated with a distinct, phase-dependent gene expression profile. *The Journal of surgical research* 178: 72-80, 2012.
18. **Hariharan N, Ikeda Y, Hong C, Alcendor RR, Usui S, Gao S, Maejima Y, and Sadoshima J**. Autophagy plays an essential role in mediating regression of hypertrophy during unloading of the heart. *PloS one* 8: e51632, 2013.
19. **Byrne NJ, Levasseur J, Sung MM, Masson G, Boisvenue J, Young ME, and Dyck JR**. Normalization of cardiac substrate utilization and left ventricular hypertrophy precede functional recovery in heart failure regression. *Cardiovasc Res* 110: 249-257, 2016.
20. **Friddle CJ, Koga T, Rubin EM, and Bristow J**. Expression profiling reveals distinct sets of genes altered during induction and regression of cardiac hypertrophy. *Proc Natl Acad Sci U S A* 97: 6745-6750, 2000.
21. **Kitagawa Y, Yamashita D, Ito H, and Takaki M**. Reversible effects of isoproterenol-induced hypertrophy on in situ left ventricular function in rat hearts. *American journal of physiology Heart and circulatory physiology* 287: H277-285, 2004.
22. **Saadane N, Alpert L, and Chalifour LE**. Expression of immediate early genes, GATA-4, and Nkx-2.5 in adrenergic-induced cardiac hypertrophy and during regression in adult mice. *Br J Pharmacol* 127: 1165-1176, 1999.
23. **Petrov G, Regitz-Zagrosek V, Lehmkuhl E, Krabatsch T, Dunkel A, Dandel M, Dworatzek E, Mahmoodzadeh S, Schubert C, Becher E, Hampl H, and Hetzer R**. Regression of myocardial hypertrophy after aortic valve replacement: faster in women? *Circulation* 122: S23-28, 2010.
24. **Kararigas G, Dworatzek E, Petrov G, Summer H, Schulze TM, Baczko I, Knosalla C, Golz S, Hetzer R, and Regitz-Zagrosek V**. Sex-dependent regulation of fibrosis and inflammation in human left ventricular remodelling under pressure overload. *European journal of heart failure* 16: 1160-1167, 2014.
25. **Miyagawa S, Toda K, Nakamura T, Yoshikawa Y, Fukushima S, Saito S, Yoshioka D, Saito T, and Sawa Y**. Building a bridge to recovery: the pathophysiology of LVAD-induced reverse modeling in heart failure. *Surgery today* 46: 149-154, 2016.
26. **Tao W, Plecka-Östlund M, Lu Y, Mattsson F, and Lagergren J**. Causes and risk factors for mortality within 1 year after obesity surgery in a population-based cohort study. *Surgery for Obesity and Related Diseases* 11: 399-405, 2015.
27. **Trexler CL, Odell AT, Jeong MY, Dowell RD, and Leinwand LA**. Transcriptome and Functional Profile of Cardiac Myocytes Is Influenced by Biological Sex. *Circulation Cardiovascular genetics* 10: 2017.
28. **Haines CD, Harvey PA, and Leinwand LA**. Estrogens mediate cardiac hypertrophy in a stimulus-dependent manner. *Endocrinology* 153: 4480-4490, 2012.
29. **Snider P, Standley KN, Wang J, Azhar M, Doetschman T, and Conway SJ**. Origin of cardiac fibroblasts and the role of periostin. *Circulation research* 105: 934-947, 2009.
30. **Mullen AC, Orlando DA, Newman JJ, Loven J, Kumar RM, Bilodeau S, Reddy J, Guenther MG, DeKoter RP, and Young RA**. Master transcription factors determine cell-type-specific responses to TGF-beta signaling. *Cell* 147: 565-576, 2011.
31. **Lijnen PJ, Petrov VV, and Fagard RH**. Induction of cardiac fibrosis by transforming growth factor-beta(1). *Molecular genetics and metabolism* 71: 418-435, 2000.
32. **Clarke K, and Ward LC**. Protein synthesis in the early stages of cardiac hypertrophy. *The International journal of biochemistry* 15: 1267-1271, 1983.
33. **Mussbacher M, Stessel H, Wölkart G, Haemmerle G, Zechner R, Mayer B, and Schrammel A**. Role of the ubiquitin-proteasome system in cardiac dysfunction of adipose triglyceride lipase-deficient mice. *Journal of molecular and cellular cardiology* 77: 11-19, 2014.
34. **Pacurari M, Kafoury R, Tchounwou PB, and Ndebele K**. The Renin-Angiotensin-aldosterone system in vascular inflammation and remodeling. *International journal of inflammation* 2014: 689360-689360, 2014.
35. **Johnson DM, and Antoons G**. Arrhythmogenic Mechanisms in Heart Failure: Linking β-Adrenergic Stimulation, Stretch, and Calcium. *Frontiers in Physiology* 9: 2018.
36. **Trimarco B, De Luca N, Cuocolo A, Ricciardelli B, Rosiello G, Lembo G, and Volpe M**. Beta blockers and left ventricular hypertrophy in hypertension. *American heart journal* 114: 975-983, 1987.

37. **Karbassi E, Monte E, Chapski DJ, Lopez R, Rosa Garrido M, Kim J, Wisniewski N, Rau CD, Wang JJ, Weiss JN, Wang Y, Lusis AJ, and Vondriska TM**. Relationship of disease-associated gene expression to cardiac phenotype is buffered by genetic diversity and chromatin regulation. *Physiological genomics* 48: 601-615, 2016.
38. **Faulx MD, Ernsberger P, Vatner D, Hoffman RD, Lewis W, Strachan R, and Hoit BD**. Strain-dependent beta-adrenergic receptor function influences myocardial responses to isoproterenol stimulation in mice. *American journal of physiology Heart and circulatory physiology* 289: H30-36, 2005.
39. **Rau CD, Wang J, Avetisyan R, Romay MC, Martin L, Ren S, Wang Y, and Lusis AJ**. Mapping genetic contributions to cardiac pathology induced by Beta-adrenergic stimulation in mice. *Circulation Cardiovascular genetics* 8: 40-49, 2015.
40. **Qi G, Jia L, Li Y, Bian Y, Cheng J, Li H, Xiao C, and Du J**. Angiotensin II infusion-induced inflammation, monocytic fibroblast precursor infiltration, and cardiac fibrosis are pressure dependent. *Cardiovascular toxicology* 11: 157-167, 2011.
41. **McLellan MA, Skelly DA, Dona MSI, Squiers GT, Farrugia GE, Gaynor TL, Cohen CD, Pandey R, Diep H, Vinh A, Rosenthal NA, and Pinto AR**. High-Resolution Transcriptomic Profiling of the Heart During Chronic Stress Reveals Cellular Drivers of Cardiac Fibrosis and Hypertrophy. *Circulation* 142: 1448-1463, 2020.
42. **Blenck CL, Harvey PA, Reckelhoff JF, and Leinwand LA**. The Importance of Biological Sex and Estrogen in Rodent Models of Cardiovascular Health and Disease. *Circulation research* 118: 1294-1312, 2016.
43. **Walker CJ, Schroeder ME, Aguado BA, Anseth KS, and Leinwand LA**. Matters of the heart: Cellular sex differences. *J Mol Cell Cardiol* 160: 42-55, 2021.
44. **Peter AK, Walker CJ, Ceccato T, Trexler CL, Ozeroff CD, Lugo KR, Perry AR, Anseth KS, and Leinwand LA**. Cardiac Fibroblasts Mediate a Sexually Dimorphic Fibrotic Response to beta-Adrenergic Stimulation. *Journal of the American Heart Association* 10: e018876, 2021.
45. **Mutlak M, and Kehat I**. Extracellular signal-regulated kinases 1/2 as regulators of cardiac hypertrophy. *Frontiers in pharmacology* 6: 149-149, 2015.
46. **Sanada S, Node K, Minamino T, Takashima S, Ogai A, Asanuma H, Ogita H, Liao Y, Asakura M, Kim J, Hori M, and Kitakaze M**. Long-acting Ca2+ blockers prevent myocardial remodeling induced by chronic NO inhibition in rats. *Hypertension (Dallas, Tex : 1979)* 41: 963-967, 2003.
47. **Li H, He C, Feng J, Zhang Y, Tang Q, Bian Z, Bai X, Zhou H, Jiang H, Heximer SP, Qin M, Huang H, Liu PP, and Huang C**. Regulator of G protein signaling 5 protects against cardiac hypertrophy and fibrosis during biomechanical stress of pressure overload. *Proc Natl Acad Sci U S A* 107: 13818-13823, 2010.
48. **Gottlieb RA, Andres AM, Sin J, and Taylor DP**. Untangling autophagy measurements: all fluxed up. *Circulation research* 116: 504-514, 2015.
49. **Zhu H, Tannous P, Johnstone JL, Kong Y, Shelton JM, Richardson JA, Le V, Levine B, Rothermel BA, and Hill JA**. Cardiac autophagy is a maladaptive response to hemodynamic stress. *The Journal of clinical investigation* 117: 1782-1793, 2007.
50. **Pfeifer U, Fohr J, Wilhelm W, and Dammrich J**. Short-term inhibition of cardiac cellular autophagy by isoproterenol. *J Mol Cell Cardiol* 19: 1179-1184, 1987.
51. **Nakai A, Yamaguchi O, Takeda T, Higuchi Y, Hikoso S, Taniike M, Omiya S, Mizote I, Matsumura Y, Asahi M, Nishida K, Hori M, Mizushima N, and Otsu K**. The role of autophagy in cardiomyocytes in the basal state and in response to hemodynamic stress. *Nature medicine* 13: 619-624, 2007.
52. **Taneike M, Yamaguchi O, Nakai A, Hikoso S, Takeda T, Mizote I, Oka T, Tamai T, Oyabu J, Murakawa T, Nishida K, Shimizu T, Hori M, Komuro I, Takuji Shirasawa TS, Mizushima N, and Otsu K**. Inhibition of autophagy in the heart induces age-related cardiomyopathy. *Autophagy* 6: 600-606, 2010.
53. **Shinmura K, Tamaki K, Sano M, Murata M, Yamakawa H, Ishida H, and Fukuda K**. Impact of long-term caloric restriction on cardiac senescence: caloric restriction ameliorates cardiac diastolic dysfunction associated with aging. *J Mol Cell Cardiol* 50: 117-127, 2011.

Figure Legends

Figure 1: Pathological cardiac hypertrophy and regression depend on the hypertrophic trigger and are modulated by sex. A. Experimental set-up. Mice were treated with Vehicle control, Ang II or Iso for 7 days, administered through an osmotic pump. Pumps were removed and regression was studied at various time-points. B. LV/TL in males and females compared to vehicle control group. N=4-8/group. LV/TL Left Ventricle Weight/Tibia Length; P = Post Hypertrophy Day. Mean ± SEM. One-way ANOVA Post hoc-Uncorrected Fisher's LSD. *p<0.05, *** p<0.0001 significance. C. Plots of gene expression measured by RNA sequencing comparing post-removal day 1 (P1) and hypertrophy in males and females treated with Ang II (above) and Iso (below). D. Venn diagram showing common differentially expressed genes among all groups. E. Biological functions identified using ingenuity pathway analysis (IPA) on the 45 genes differentially expressed genes in common to all groups.

Figure 2: Fibrotic signaling involved upon removal of hypertrophic trigger. A. Heatmap showing the top canonical pathways identified by Ingenuity Pathway Analysis (IPA) that are enriched at post-removal day 1 (P1) in male and female mice treated for 7 days with Ang II or Iso. Complete list in Fig S3. TGFβ1 in Male Iso is the most significant upstream regulator predicted (p=4.99e-61) compared to any other regulator in all groups. IPA predicts the inhibition of TGFβ1 regulator for Male Iso (z-score = -6.085). C. Selected differentially expressed genes regulated by TGFβ1 in male Iso at P1 and normalized by hypertrophy. D. Hydroxyproline content measured in all groups. Seven 7 days of treatment with hypertrophic trigger did not induced increase of collagen deposition (Vehicle vs. Hypertrophy). Significant increase of collagen deposition was observed after removal of hypertrophic stimuli as compared to hypertrophy. Mean ± SEM. One-way ANOVA Post hoc-Uncorrected Fisher's LSD. *p<0.05, ** p<0.01, *** p<0.0001 significance N=4-8/group.

Figure 3: TGFβ1 signaling. A. Scheme showing the TGFβ1 signaling pathways via SMAD, AKT, ERK, p38. B. Western blot of SMAD2/3 phosphorylation C. Western blot of Akt phosphorylation. There was little regulation of Akt in response to Ang II or Iso in males or females. Protein quantifications were normalized to Vinculin. D. Western blot of ERK1/2 was activated in male mice with Ang II or Iso, which decreased after stimulus removal. ERK1/2 was not activated in female mice with Ang II or Iso, but was decreased after the removal of Iso. E. Western blot of p38 phosphorylation. Protein quantifications were normalized to Vinculin. Mean ± SEM. One-way ANOVA Post hoc-Uncorrected Fisher's LSD. *p<0.05, ** p<0.01, *** p<0.0001 significance; N=4-8/group. Hypertrophy group compared to Vehicle control; P1, P4, and P7 compared to Hypertrophy.

Figure 4: Protein degradation pathways. A. Measurements of proteasome. Proteasome increased in males in response to Ang II and Iso; then increased further in response to Iso removal but decreased after Ang II removal. Proteasome activity was unchanged in female mice. B. Autophagy activity did not significantly changed in male and female Ang II. Autophagy increased after the removal of Iso in male mice. In female mice, autophagy activity decreased with Iso; then increased after

Iso removal. Mean ± SEM. One-way ANOVA Post hoc-Uncorrected Fisher's LSD. *$p<0.05$, ** $p<0.01$, *** $p<0.0001$ significance; N=4-8/group. Hypertrophy group compared to Vehicle control; P1, P4, and P7 compared to hypertrophy.

Figure 5: Summary table of significant results. Arrows indicate $p<0.05$. Red arrow indicates upregulation and green arrow downregulation.

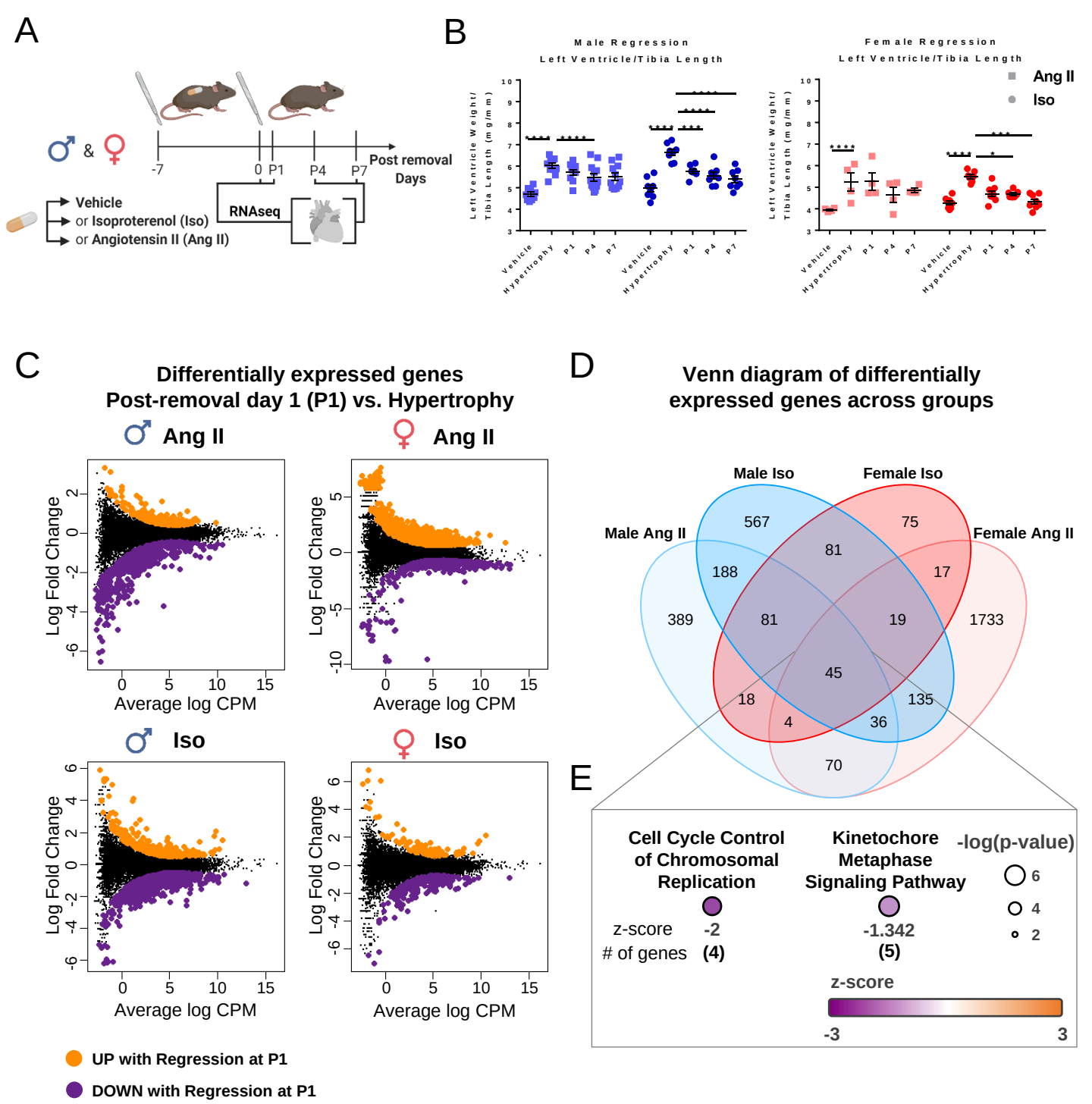
A
♂ & ♀
-7
0 P1
P4
P7
Post removal Days
Vehicle
or Isoproterenol (Iso)
or Angiotensin II (Ang II)
RNAseq
B
Male Regression
Left Ventricle/Tibia Length
Female Regression
Left Ventricle/Tibia Length
Left Ventricle Weight/ Tibia Length (mg/mm)
Ang II
Iso
Vehicle
Hypertrophy
P1
P4
P7
C
Differentially expressed genes
Post-removal day 1 (P1) vs. Hypertrophy
♂ Ang II
♀ Ang II
♂ Iso
♀ Iso
Log Fold Change
Average log CPM
UP with Regression at P1
DOWN with Regression at P1
D
Venn diagram of differentially expressed genes across groups
Male Iso
Female Iso
Male Ang II
Female Ang II
567
75
81
188
17
389
81
19
1733
45
18
135
4
36
70
E
Cell Cycle Control of Chromosomal Replication
Kinetochore Metaphase Signaling Pathway
-log(p-value)
6
4
2
z-score -2
# of genes (4)
-1.342
(5)
z-score
-3
3

Figure 1

A

Enriched signaling pathways

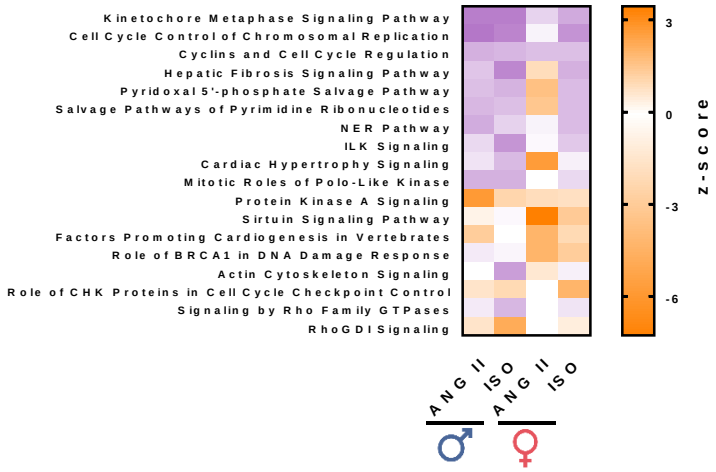

B

Prediction of TGFβ as upstream regulator at P1 vs. Hypertrophy in all groups

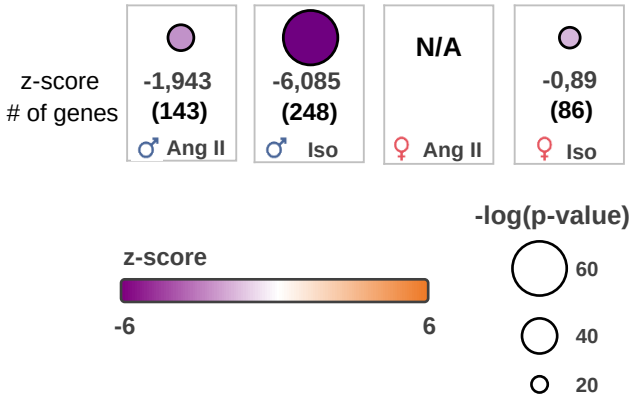

C

Selected differentially expressed genes in Male Iso at P1 vs. Hypertrophy regulated by TGFβ

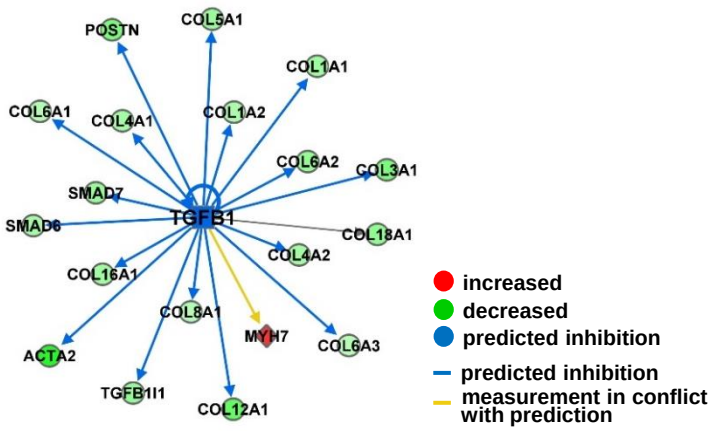

D

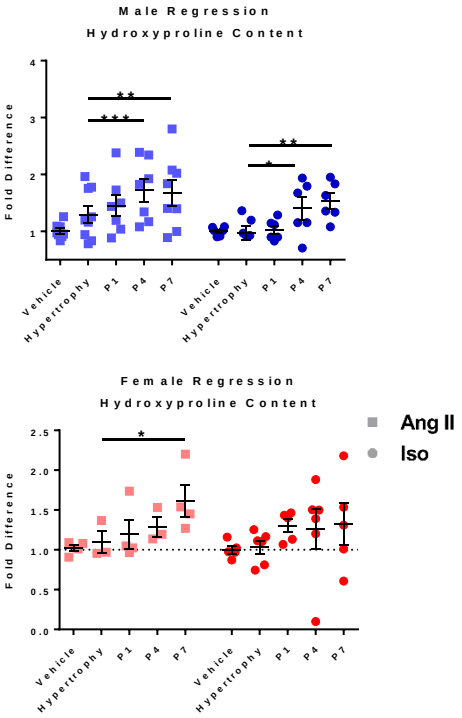

Figure 2

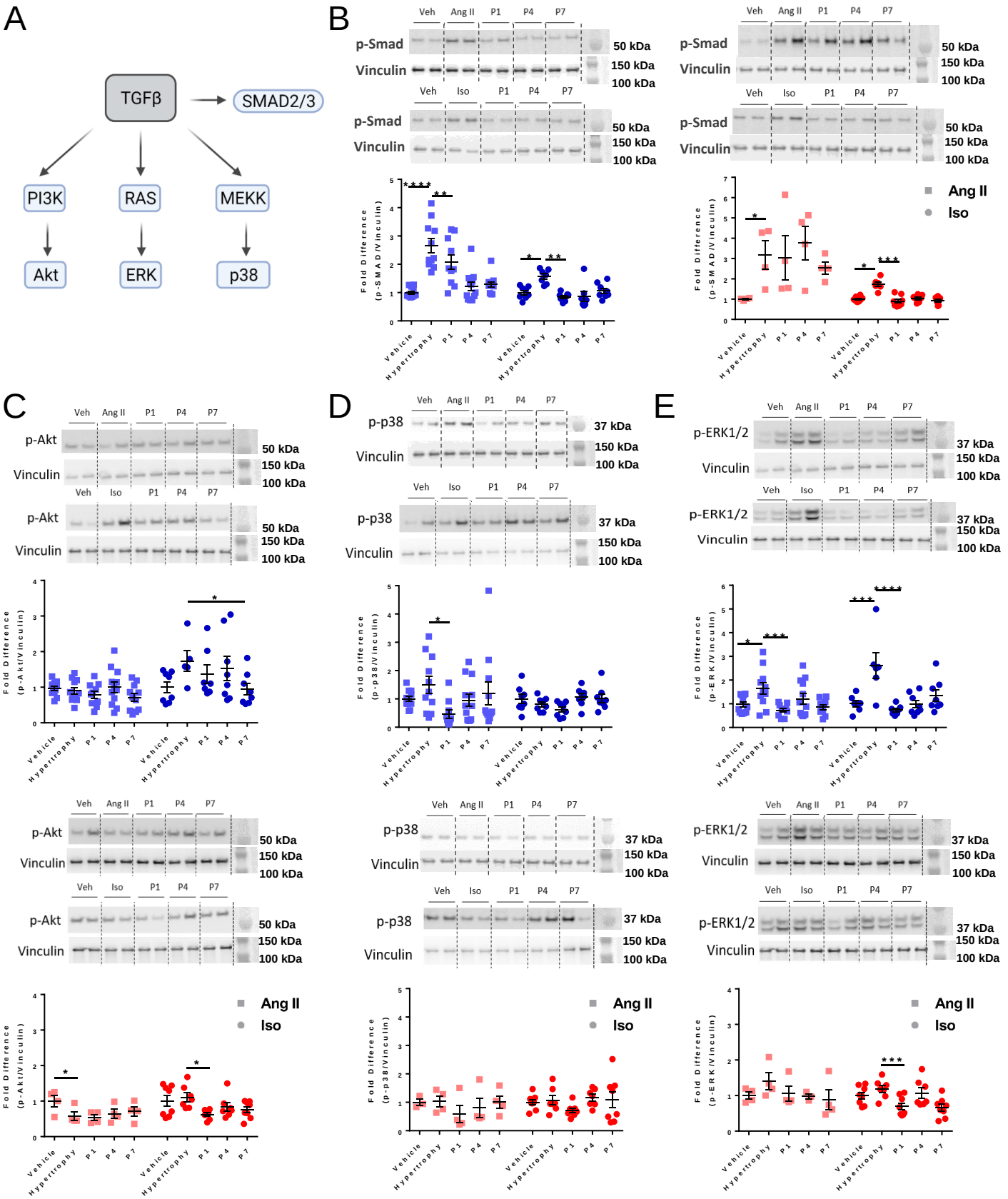
A
TGFβ
SMAD2/3
PI3K
RAS
MEKK
Akt
ERK
p38
B
p-Smad
Vinculin
Veh
Ang II
Iso
P1
P4
P7
50 kDa
150 kDa
100 kDa
Fold Difference (p-SMAD/Vinculin)
Vehicle
Hypertrophy
Ang II
Iso
C
p-Akt
Fold Difference (p-Akt/Vinculin)
D
p-p38
Fold Difference (p-p38/Vinculin)
37 kDa
E
p-ERK1/2
Fold Difference (p-ERK/Vinculin)

Figure 3

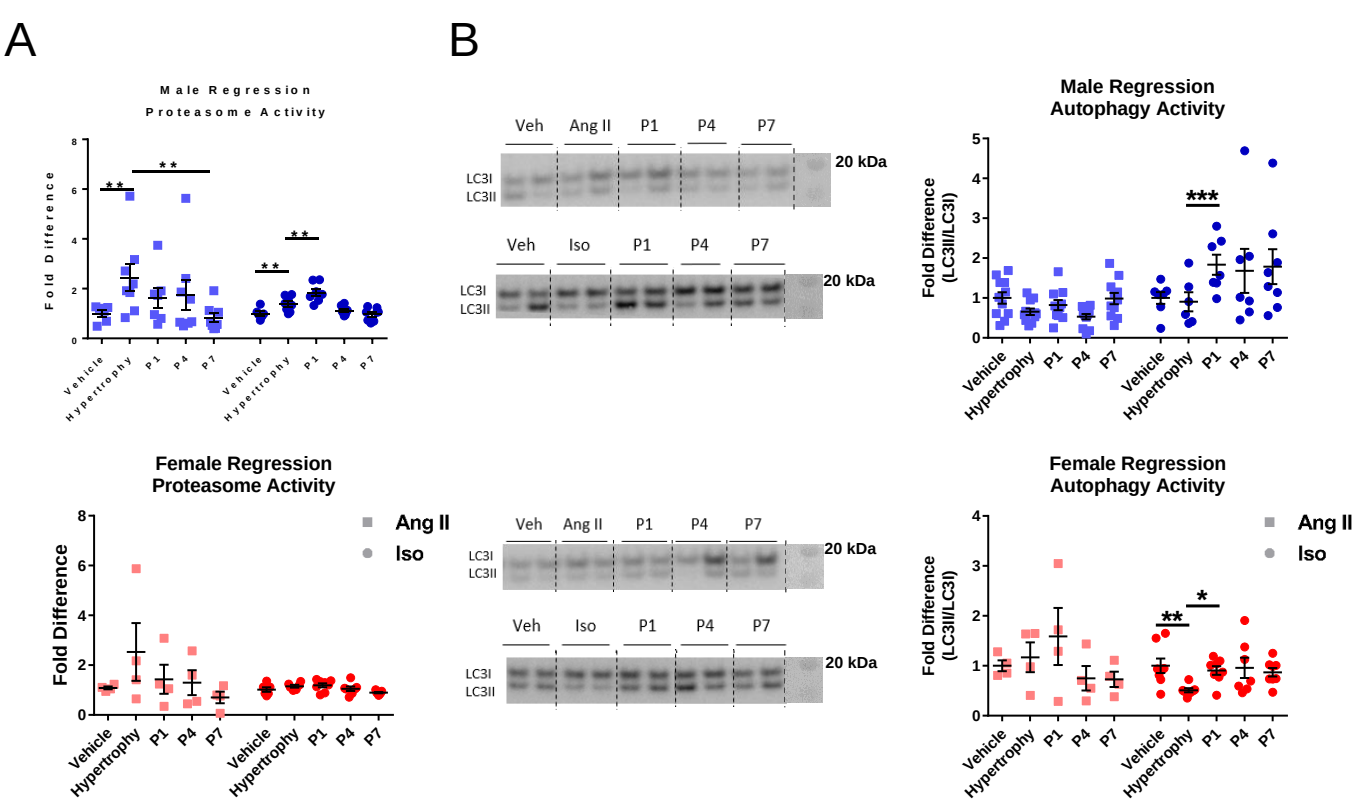
A
B
Male Regression
Proteasome Activity
Fold Difference
Vehicle
Hypertrophy
P1
P4
P7
Veh
Ang II
Iso
LC3I
LC3II
20 kDa
Male Regression
Autophagy Activity
Fold Difference
(LC3II/LC3I)
Female Regression
Proteasome Activity
Ang II
Iso
Female Regression
Autophagy Activity

Figure 4

		AngII		Iso	
		Males	Females	Males	Females
LV/TL	Hyp vs. Veh	↑	↑	↑	↑
	P1 vs Hyp	–	–	↓	↓
	P4 vs Hyp	↓	–	↓	↓
	P7 vs Hyp	–	–	↓	↓
Hydroxiproline	Hyp vs. Veh	–	–	–	–
	P1 vs Hyp	–	–	–	–
	P4 vs Hyp	↑	–	↑	–
	P7 vs Hyp	↑	↑	↑	–
Col1a1	Hyp vs. Veh	↑	↑	↑	↑
	P1 vs Hyp	–	–	–	–
	P4 vs Hyp	↓	–	↓	↓
	P7 vs Hyp	↓	–	–	–
Postn	Hyp vs. Veh	↑	–	↑	↑
	P1 vs Hyp	–	↑	↓	↓
	P4 vs Hyp	↓	–	↓	↓
	P7 vs Hyp	↓	–	↓	↓
p-SMAD2/3	Hyp vs. Veh	↑	↑	↑	↑
	P1 vs Hyp	↓	–	↓	↓
	P4 vs Hyp	↓	–	↓	↓
	P7 vs Hyp	↓	–	↓	↓
p-Akt	Hyp vs. Veh	–	↓	–	–
	P1 vs Hyp	–	–	–	↓
	P4 vs Hyp	–	–	–	–
	P7 vs Hyp	–	–	↓	–
p-p38	Hyp vs. Veh	–	–	–	–
	P1 vs Hyp	↓	–	–	–
	P4 vs Hyp	–	–	–	–
	P7 vs Hyp	–	–	–	–
p-ERK1/2	Hyp vs. Veh	↑	–	↑	–
	P1 vs Hyp	↓	–	↓	↓
	P4 vs Hyp	–	–	↓	–
	P7 vs Hyp	↓	–	↓	↓
Proteasome	Hyp vs. Veh	↑	–	↑	–
	P1 vs Hyp	–	–	↑	–
	P4 vs Hyp	↓	–	↓	–
	P7 vs Hyp	↓	–	↓	–
Autophagy	Hyp vs. Veh	–	–	–	↓
	P1 vs Hyp	–	–	↑	↑
	P4 vs Hyp	–	–	↑	↑
	P7 vs Hyp	–	–	↑	↑

Figure 5